DYNAMIC FEATURES AND IDENTIFICATION OF REGIONAL SEISMIC SIGNALS FROM DEAD SEA CALIBRATION SHOTS

Yefim Gitterman and Rami Hofstetter

Geophysical Institute of Israel

Sponsored by The Defense Threat Reduction Agency

Contract No.DSWA01-97-C-0151

ABSTRACT

Three large-scale underwater chemical explosions were conducted on November 8-11, 1999 in the Dead Sea. One of the main objectives of the experiment was to provide data for source characterization to improve the IMS detection, location and discrimination capabilities.

The explosions were recorded by the Israel Seismic Network (ISN) including 23 short-period (SP) stations, two auxiliary IMS broadband (BB) stations MRNI and EIL, BB station JER, and three temporary BB stations deployed at sites of the planned Israeli CNF stations.

The magnitude values, determined from SP recordings, fit well the empirical relationship obtained from previous explosions: $M_L = 0.285 + \log_{10}W(kg)$, confirming a high seismic efficiency of the shots. The efficiency was also estimated by determination of energy of seismic waves recorded at local seismic stations relative to the explosives energy.

A clear spectral modulation, caused by the bubble pulsation effect, is observed in all SP and BB seismograms. The bubble periods, determined from the harmonic series on smoothed spectra of ISN seismograms, are in good agreement with the modified Willis' (1963) empirical equation: $T_b=2.1*W^{1/3}/(P_0+d*\square)^{5/6}$, where P_0 is the pressure at the sea level (10.778 m of water column), the shot depth d=70 m, water density $\square$=1.236g/cm^3.

Date	Charge W, kg	Local (duration) magnitude M_L		Bubble period T_b, sec	
		Predicted	Observed	Predicted	Observed
08.11.99	500	3.0	3.1	0.367	0.383
10.11.99	2060	3.6	3.6	0.589	0.561
11.11.99	5000	4.0	3.9	0.791	0.782

Identification of the seismic signals from underwater explosions is based on spectral features of recordings: spectra coherency at different stations, due to the bubbling modulation and low-frequency seismic energy. Discrimination analysis was done by spectral energy ratio (1-3Hz)/(6-8Hz) and semblance (1-12Hz) characteristics, using local SP and BB stations data of the explosions and nearby earthquakes with comparable magnitudes. The methods provided reliable discrimination between earthquakes and explosions in the Dead Sea region.

Key words : Dead Sea explosions, seismic energy, spectra, bubble periods, semblance, spectral ratio

OBJECTIVE

The primary objective of this study is to characterize the specific seismic source for the Dead Sea calibration underwater explosions in a short distance range, to estimate the seismic efficiency of the shots, to investigate dynamic features of radiated seismic waves and provide a preliminary discrimination analysis of the explosions and nearby earthquakes.

RESEARCH ACCOMPLISHED

Local station data. The charge parameters and Ground Truth Information are presented in Gitterman and Shapira (2000). The explosions were recorded by the Israel Seismic Network (ISN), consisting of 23 SP stations, two auxiliary IMS stations MRNI and EIL, and CNF station JER (Jerusalem). Three temporary (surrogate) BB stations were deployed at sites of planned CNF stations (AMZI, MMLI and DIM). Temporary short-period seismic stations were placed along the Dead Sea coast, at the Mineral Beach (HOF, the closest point), and in the hotel area, Ein-Bokek (CRL): two 3C stations on the Hotel Carlton building and two 3C stations on the ground near the Hotel. Station locations are shown on the map on Fig. 1 Data of several Jordanian stations, presented also on the map, were obtained on-line at the Geophysical Institute of Israel.

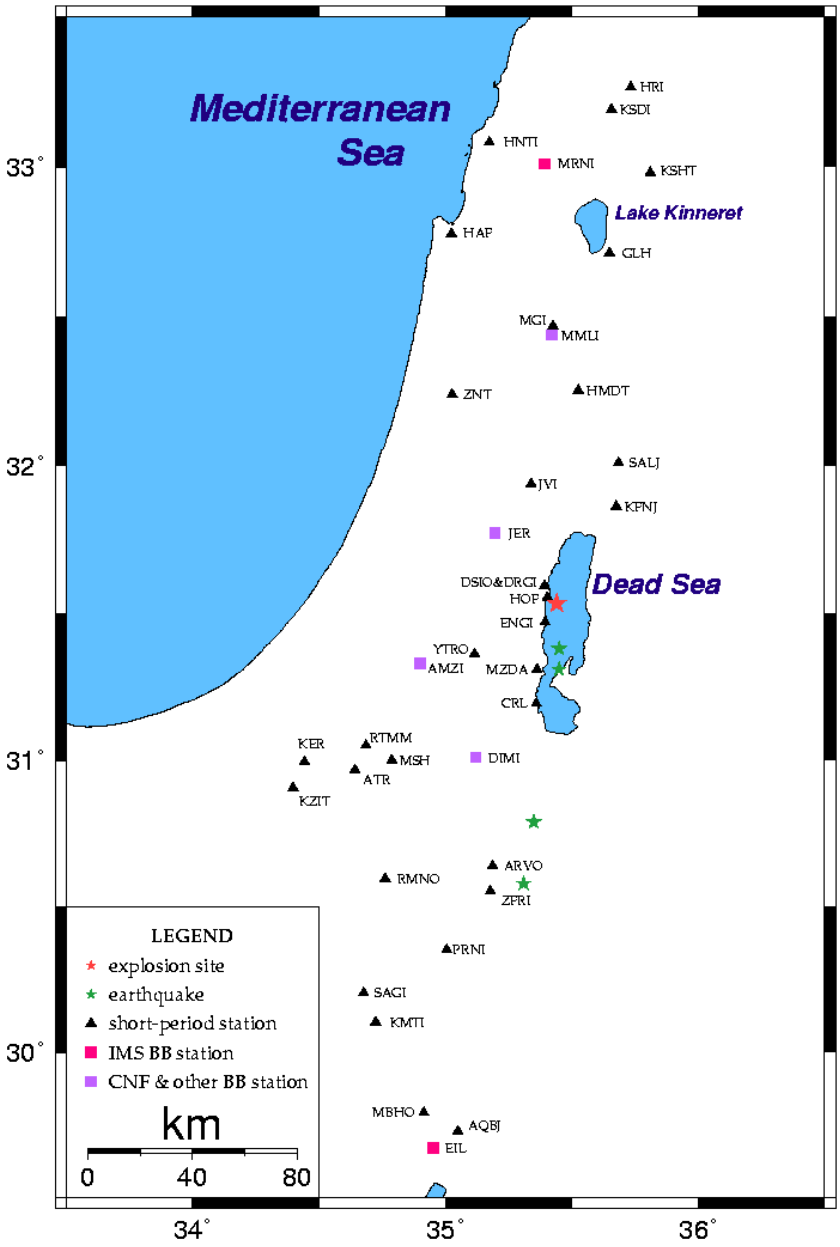

Fig. 1. Location of Israel and Jordanian seismic stations recorded the explosions.

Near-field observations. Several strong motion sensors were installed along the west coast of the Dead Sea. The maximal Peak Ground Acceleration, 0.0769g, was observed at the Mineral Beach at distance 4.2 km (Fig. 2).

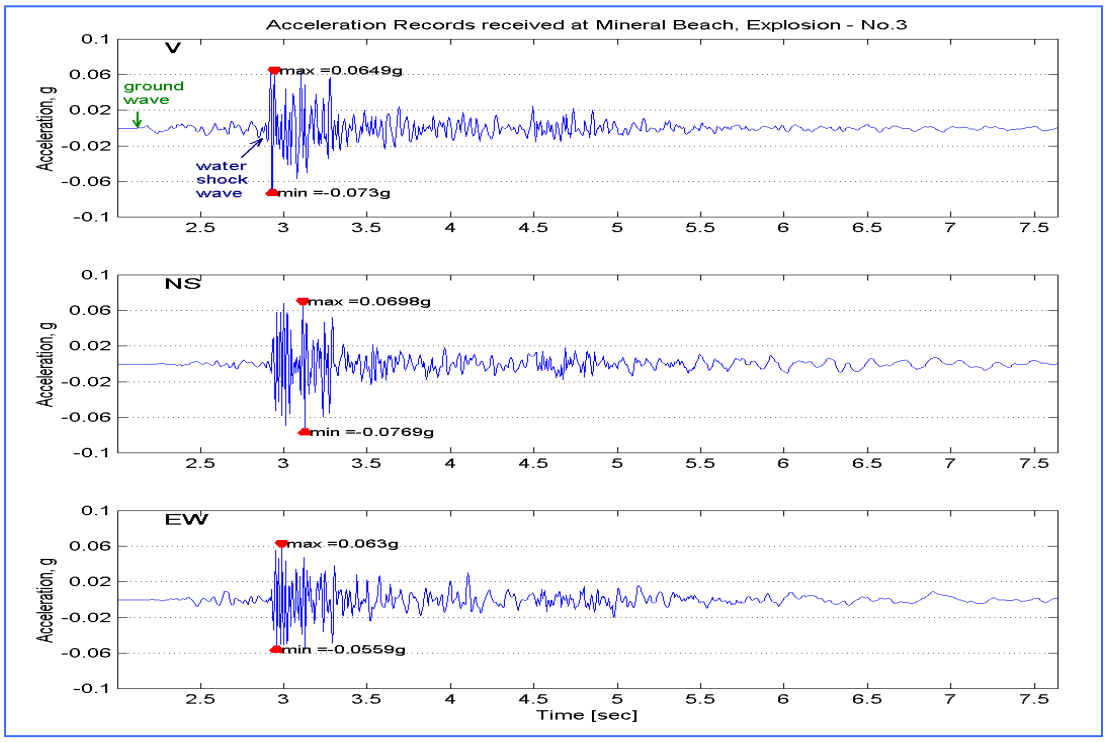

Fig.2. Accelerograms observed at Mineral Beach from the 5000 kg shot.

The high-frequency (about 40-55 Hz) and high-amplitude seismic waves, recorded by an accelerometer A-800, located in a few meters from the shore, are generated by the shock wave - sea shelf interaction. It is evident from the joint recording of a seismometer co-located with the A-800 and a nearby hydrophone placed in water (Fig.3).

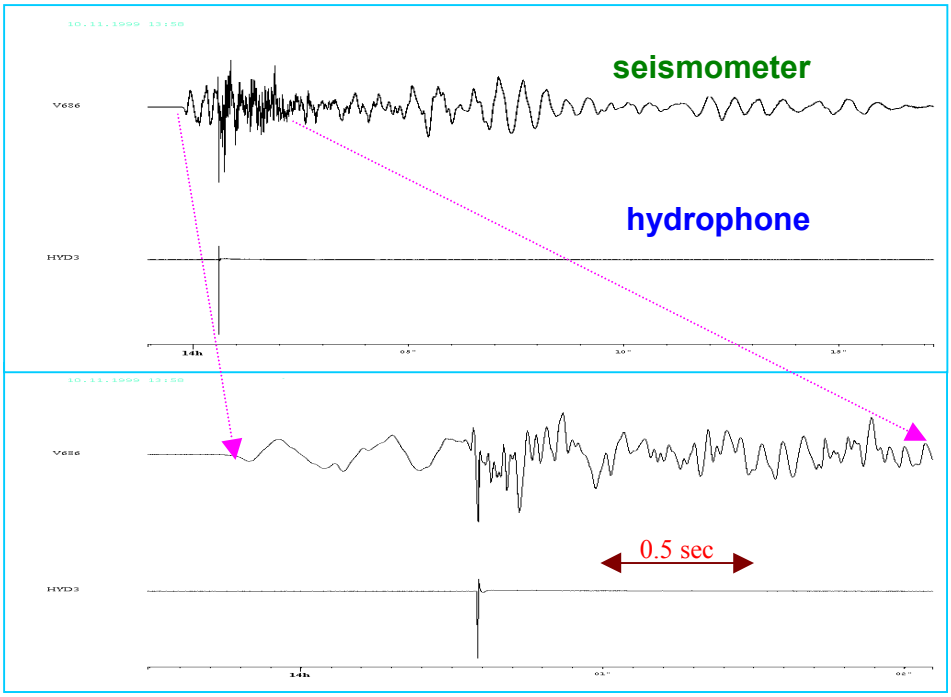

Fig. 3. Seismometer and hydrophone recording at Mineral Beach of the 2000 kg explosion.

Seismic efficiency. An increase of explosion charge weight causes an appropriate rise of radiated seismic energy, and corresponding magnitudes and signal amplitudes, as well as signal periods and wavelengths. Two small test shots (25 kg), conducted two weeks before the main series at the same location and depth, are also considered.

Table 1. Comparison of predicted and observed local magnitudes and fundamental frequencies of the calibration explosions in the Dead Sea (depth d ~ 70m).

ChargeW, kg	Local (ISN based) magnitude M_L		Frequency f_b, Hz / Bubble period T_b, sec		
	Predicted (Eq. 1)	Measured	Predicted (Eq. 3)	Measured	
				average from ISN spectral maxima	from autocorrelation analysis of IMS stations (CMR event Report, 1999)
25 (two shots)	1.7	1.7 1.9	7.20/0.139	6.50/0.154	-
500	3.0	3.1	2.72/0.367	2.61/0.383	2.70/0.37
2060	3.6	3.6	1.70/0.589	1.78/0.561	1.82/0.55
5000	4.0	3.9	1.26/0.791	1.28/0.782	1.30/0.77

Observed local (duration) magnitudes (Table 1), determined from short-period ISN recordings, correspond well to the values predicted at the design stage of the experiment by the empirical relationship (Gitterman, 1998):

$$M=0.285+\log_{10}(W, \text{kg}) \quad (1)$$

based on the 1993 series of small scale Dead Sea shots (Gitterman et al., 1998). The high magnitudes under relatively low charge weights confirm a high seismic efficiency of underwater explosions in the Dead Sea, significantly exceeding the upper limit curve for all known chemical and nuclear explosions in hard rock (Khalturin et al., 1997), presented on Fig. 4. The observed magnitudes and amplitudes of seismic waves verify that the whole charge was properly detonated in all cases.

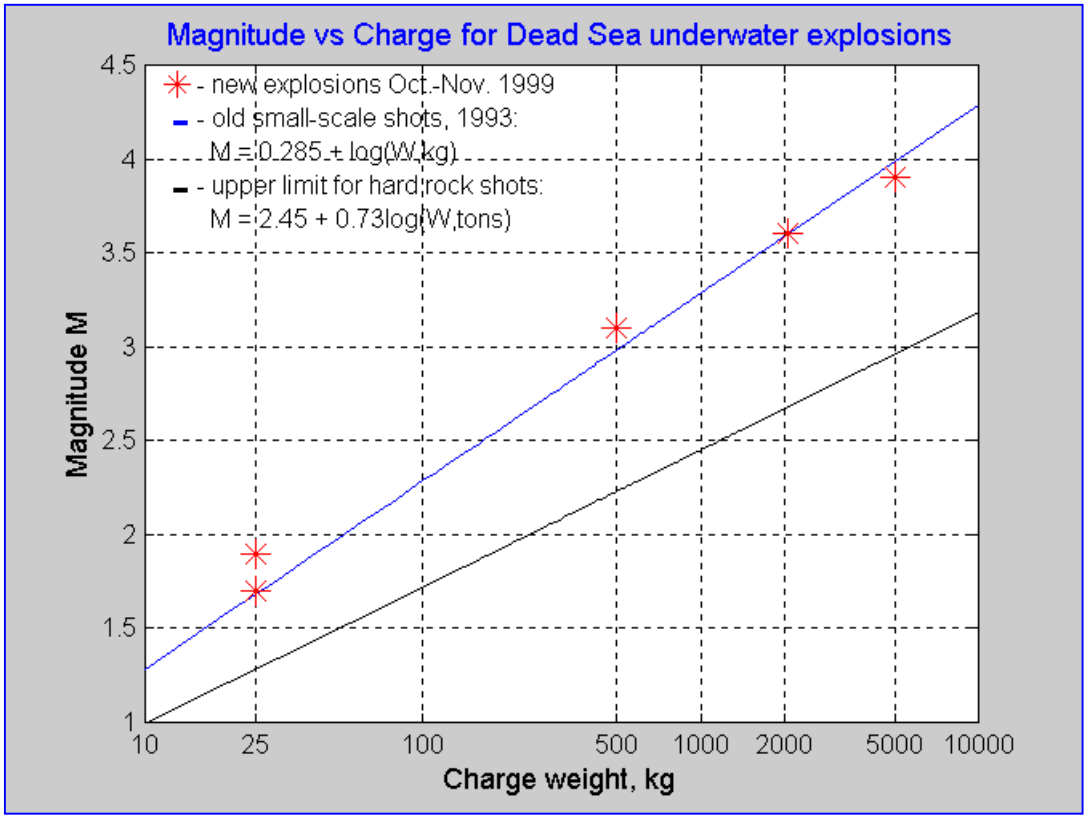

Fig. 4. Magnitude versus charge weight for the Dead Sea explosions.

Some features of seismic amplitudes and waveforms for the three explosions, observed at stations located at different distances and azimuths, are shown on Fig. 5.

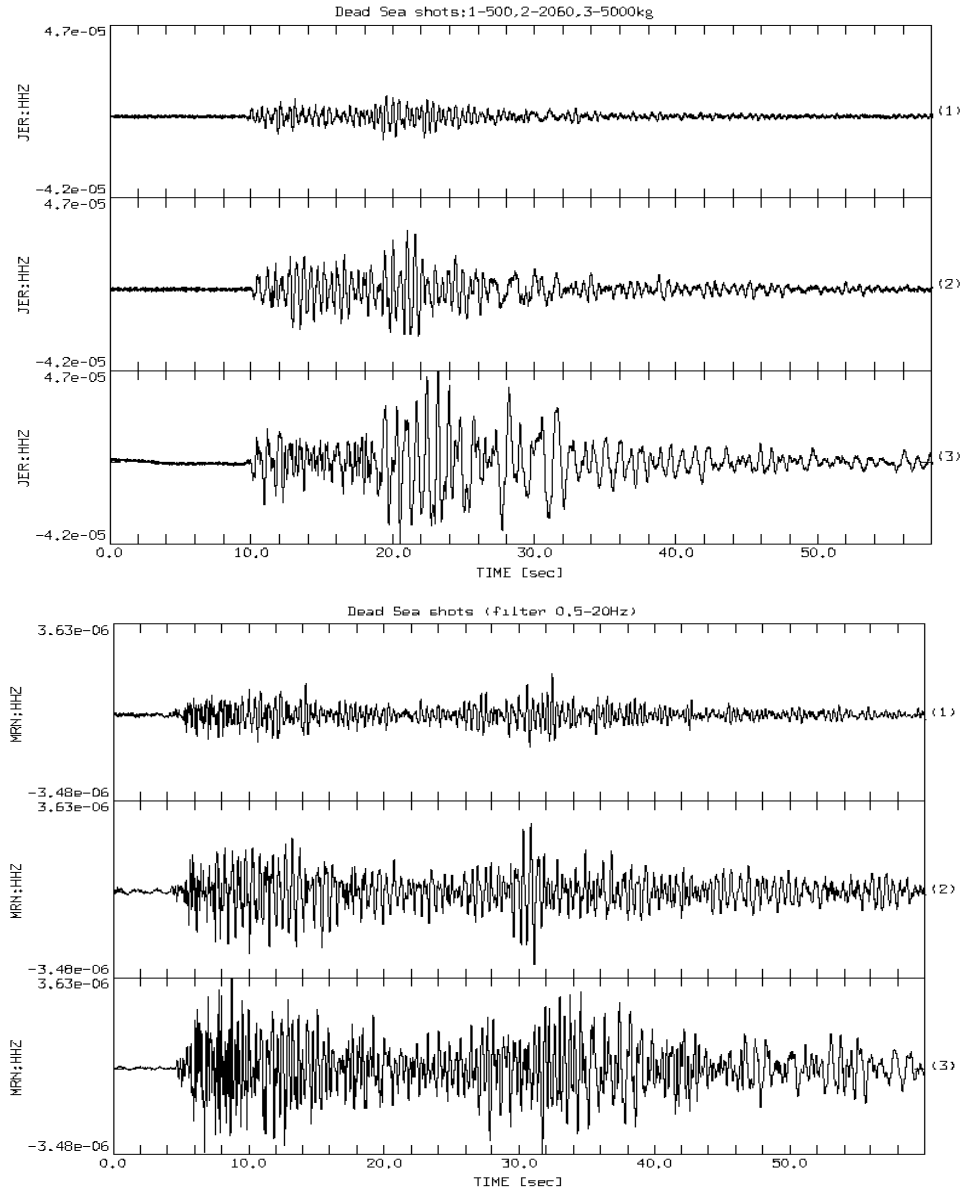

Fig. 5. Signal enhancement at BB stations JER (r=35 km) and MRNI (r=164 km) with the charge increase.

The explosion seismic efficiency was also estimated by determination of energy of seismic waves recorded at local seismic stations relative to the explosives energy. The energy release of an earthquake is an important physical quantity that describes the earthquake. Kanamori et al. (1993) presented a method for the estimation of the seismic energy, based on time-domain integration, of local and regional velocity-squared seismograms observed at TERRAscope in Southern California. They were able to obtain reliable energy estimation, since the propagation effect is of minor importance at short distances. Recently, Mayeda and Walter (1996) proposed to estimate the energy from the coda envelops using broad band data at different frequency ranges. The method of Mayeda and Walter (1996) seems to be better than that of Kanamori et al. (1993). Calibration of the region is now in progress, and once it is being achieved, a refinement of the results is expected when applying the method of Mayeda and Walter (1996). In the presented research we used the method of Kanamori et al. (1993) to estimate the seismic energy of the Dead Sea explosions.

Hofstetter and Shapira (2000) estimated the attenuation function in the short period frequency range (0.5 Hz to 10 Hz)

$$A(R) = (1.850 \pm 0.005)\ logR + (0.00460 \pm 0.00005)R\ loge + 0.05 \qquad (2)$$

where R is the hypocentral distance $R^2 = \Delta^2 + h^2$ in the distance range of $50 \le R \le 1500$ km, Δ is the epicentral distance, h is the source depth which is close to zero in our case. The standard deviation is 0.24 (or uncertainty factor of 1.7). The function (2) was utilized for estimation of the seismic energy for the Dead Sea shots, observed at several 3C short period and broad band stations of the Israel Seismic Network, including IMS and CNF stations (see Fig. 1), located at different distances (range 50-211 km) and azimuths. Fig. 6 shows the seismic efficiency, estimated as:

$$Efficiency = \frac{seismic\ \ energy}{Explosives\ \ energy}$$

where, according to the manufacturer's specification, the energy of the used Chen Amon explosives is given by $1000\text{cal/gr} = 4.2\times10^{13}$ erg/kg. The efficiency values for different stations are averaged, and the variance is also shown for different shots.

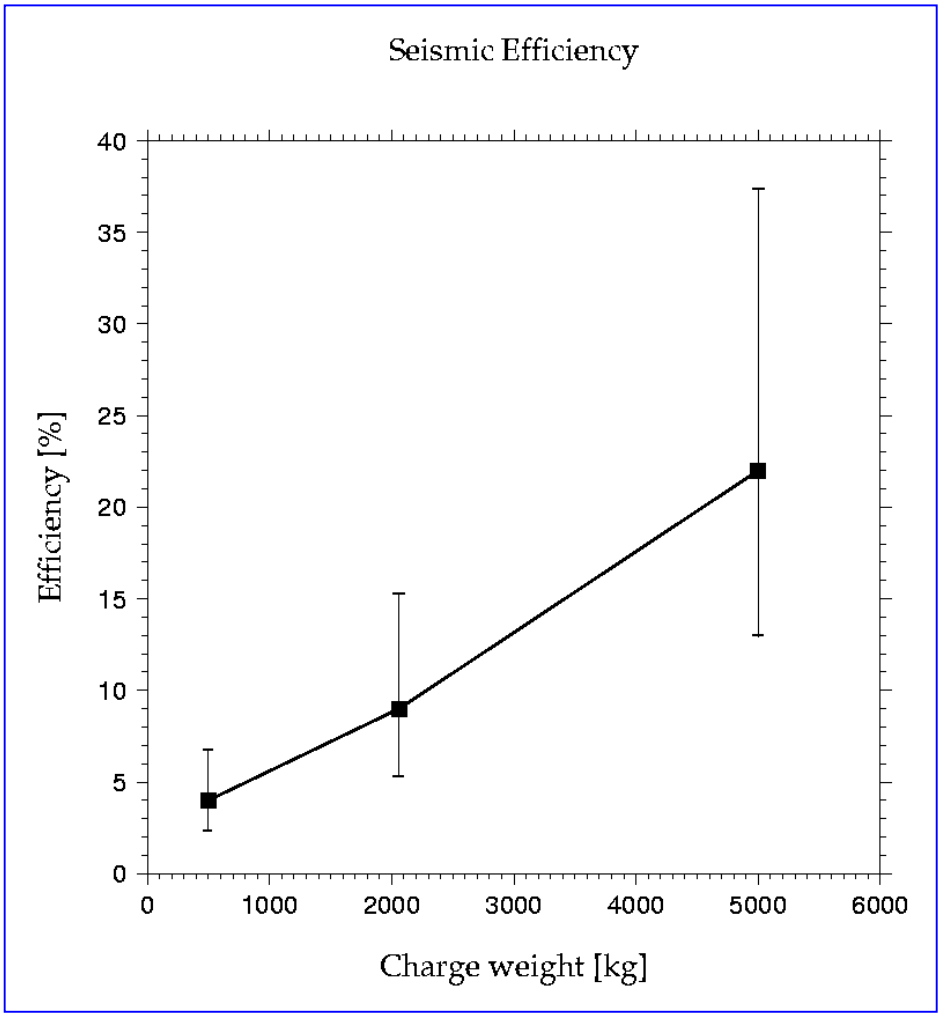

Fig. 6. Seismic efficiency of the Dead Sea calibration underwater explosions estimated from seismograms of local short period and broad band stations, located in the distance range 50-200 km.

Evidently, a large part of the explosives energy was released with uprising hot gases in the detonation vicinity, and the energy of initially radiated seismic waves was either absorbed or scattered in the media along the propagation path to a station. But it is obvious that the efficiency of the underwater explosions in the Dead Sea (especially for the largest explosions 5000 kg), is much higher than that for similar hard-rock shots, which as known reaches a few percents only (see also Fig. 4).

We suppose that the efficiency values for the shots 500 kg and 2060 kg are underestimated, nevertheless the increase trend corresponds to a lesser scattering of seismic energy on the crust inhomogeneities and a lower intrinsic dissipation of seismic energy for longer wavelengths from larger shots.

Bubbling effect and spectral modulation. The prominent azimuth and distance independent spectral modulation, caused by the bubble pulsation effect, is presented in all SP and BB seismograms. The clear frequency banding is observed in smoothed amplitude spectra of the whole signal (50-60 sec) and in spectrograms (see examples on Figures 7 and 8).

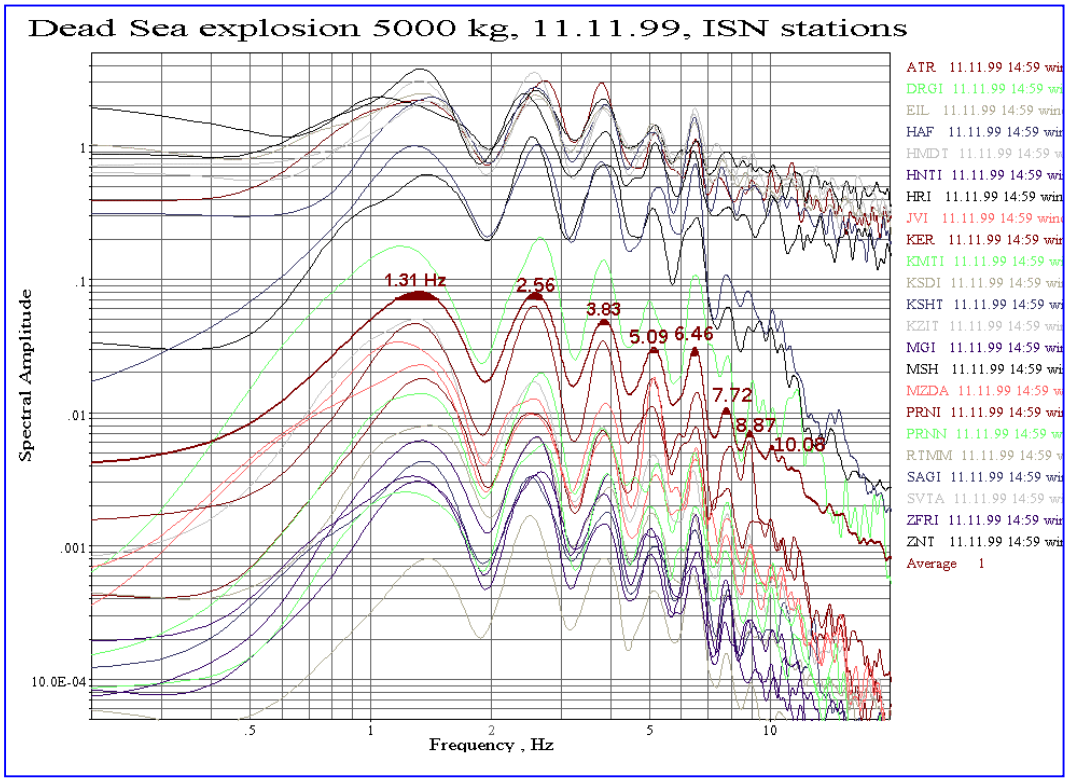

Fig. 7. Determination of the bubble frequency from smoothed averaged spectra of ISN seismograms.

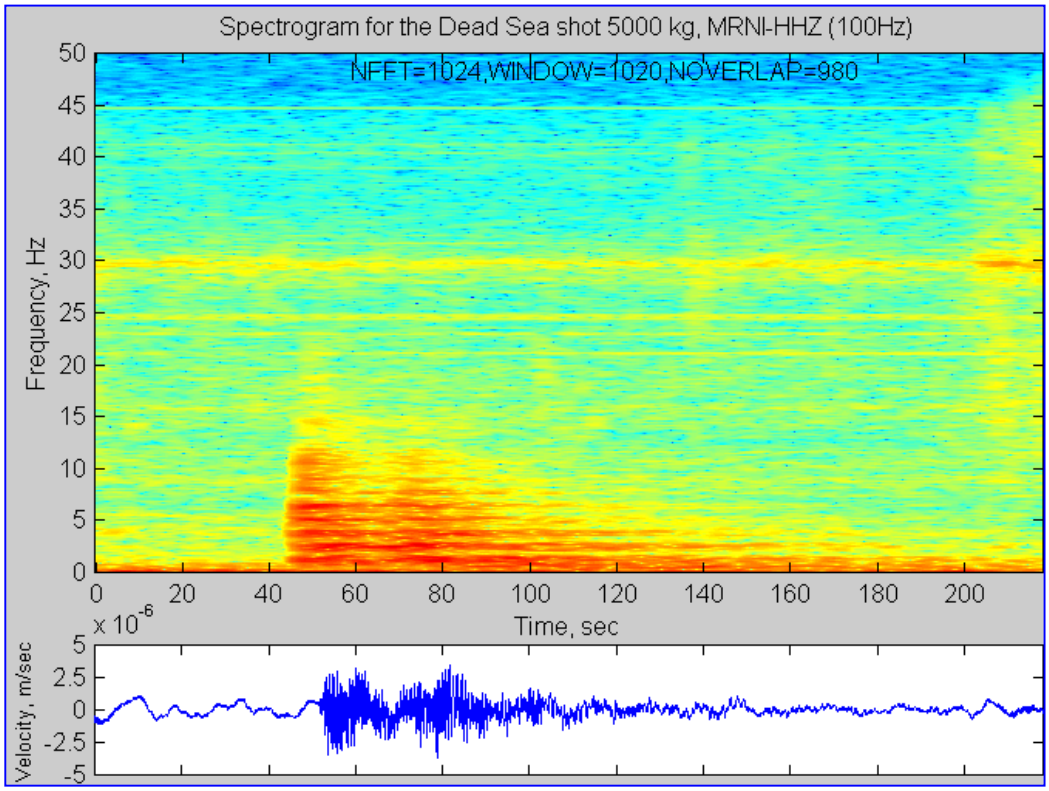

Fig. 8. Spectrogram of the largest explosion recorded at the BB IMS station MRNI (vertical component) with 100 sps (time windows 10.2 sec, shift 0.4 sec).

Spectrograms demonstrate time-independent spectral modulation with at least eight harmonic strips observed in the initial part of seismogram. The high-frequency strips are disappearing with time increasing. The low-frequency (less than 1 Hz) energy belongs to the coda of an earthquake in Turkey preceding the explosion. Obtained spectra and spectrograms show no energy at frequencies more than 10-12 Hz.

The bubble periods (and bubble frequencies), determined from the harmonic series in smoothed spectra of ISN seismograms (Fig. 7), are in good agreement with the modified Willis' (1963) empirical equation (see Table 1):

$$T_b = 2.1 * W^{1/3}/(P_0 + d * \square)^{5/6} \qquad f_b = 1/T_b \qquad (3)$$

where P_0 is the barometric pressure at the level of the Dead Sea (792 mm mercury or 10.778 m of water column during the experiment), the shot depth d = 70 m, water density $\square$=1.236g/cm^3. The observed periods are also consistent with estimations obtained from hydrophone recordings (Gitterman and Shapira, 2000), and from autocorrelation analysis of IMS stations (CMR Event Report, 1999).

Discrimination analysis. We tested the spectral classification method (Gitterman et al., 1998), which includes application to seismograms at different network stations of two spectral statistics: a) energy ratio in low and high frequency windows, averaged for several stations; b) semblance, characterizing coherency of spectral curves at network stations.

The method was applied to vertical ISN and 3C Broad Band (EIL, JER and MRNI) records of the three calibration explosions in the Dead Sea and of four earthquakes close in magnitude, location and time occurrence to the explosions. The earthquake parameters are presented in Table 2, and all analyzed events and recording stations are shown on Fig.1.

Table 2. List of earthquakes of October-November 1999, close in location and magnitude to the Dead Sea calibration shots.

Date year/month/day/hour/min/sec	Magn. M_L	X, km	Y, km	Depth, km	Latit.	Long.	Region
1999 10 04 02 04 37.6	2.8	192.4	80.2	22	31.31	35.45	Arad
1999 10 07 03 50 26.8	2.9	179.8	-0.6	9	30.58	35.31	Arava
1999 11 16 02 39 15.5	3.4	192.3	87.7	21	31.38	35.45	Arad
1999 11 16 16 57 45.0	2.7	183.0	21.7	15	30.79	35.35	Arava

Time windows of 30-40 sec, containing the whole signal, were used. The spectra are smoothed in frequency windows about 0.7 Hz, energy ratio was calculated for the (1-3 Hz)/(6-8 Hz) ranges, and semblance for the (1-12 Hz) range. For BB data the semblance is calculated in 1-9 Hz range, because only 20Hz records are available for some earthquakes.

Identification of underwater explosions is based on spectral features of recordings: spectra coherency at different stations, due to the bubbling modulation and low-frequency seismic energy. Figures 9-10 show coherent and relatively low-frequency spectra for the explosions, and non-regular and high-frequency spectra for the earthquakes. The different spectral patterns provided clear separation of the two populations of seismic events in the two-parametric space, shown on Fig. 11.

The spectral methods for discrimination between earthquakes and underwater explosions provided reliable automated identification of the Dead Sea explosions. These observations correspond well to the results from the previous series of smaller underwater explosions (16-304 kg) conducted along a profile in the Dead Sea in 1993 (Gitterman et al., 1998). In the following we are going to conduct the similar spectral discrimination analysis using data obtained at more distant short-period and BB stations.

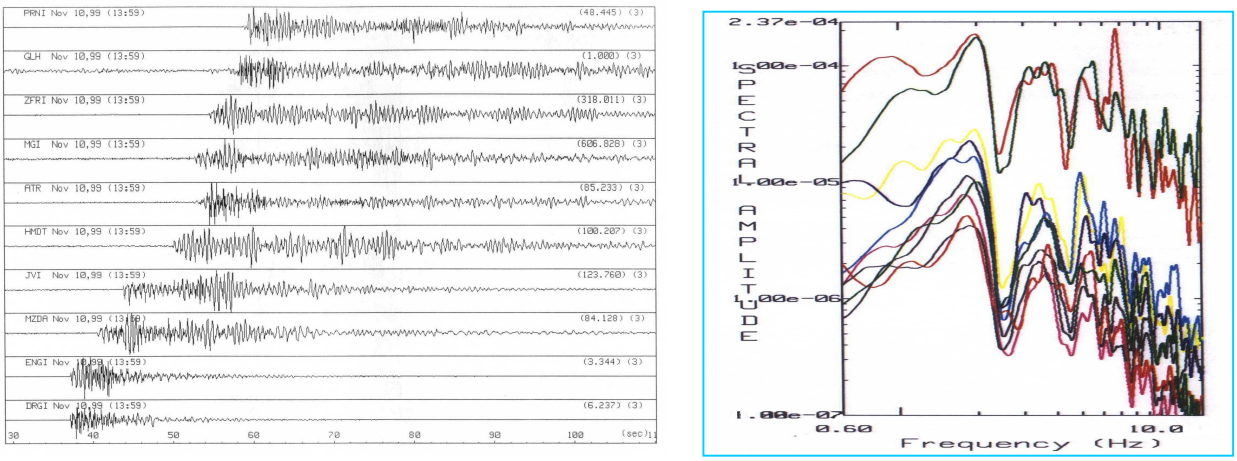

Fig. 9. Sample seismogram and spectral patterns at different ISN stations for the Dead Sea shot 2060 kg.

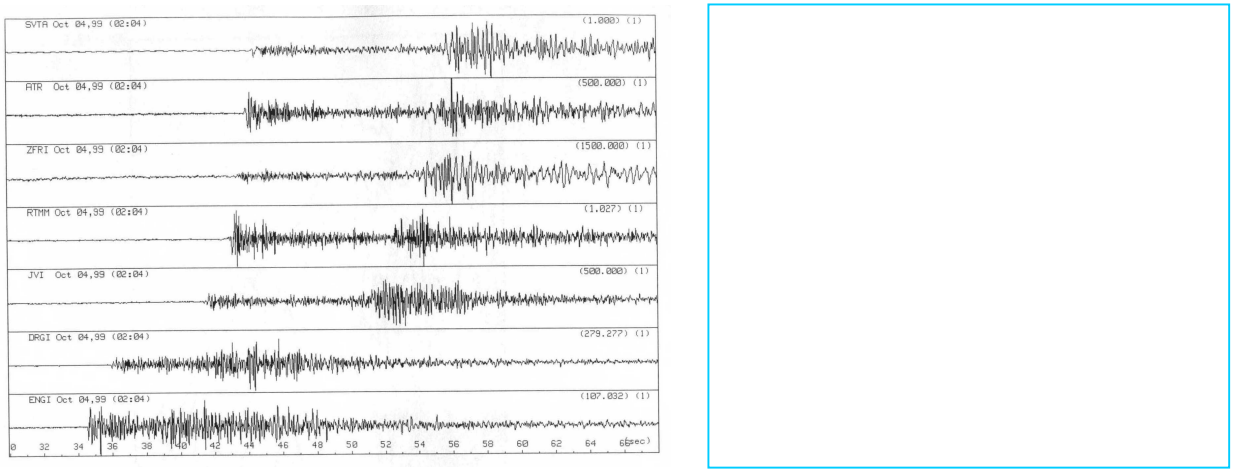

Fig. 10. Sample seismogram and spectral patterns at different ISN stations for the closest to the explosion site earthquake on 4.10.99.

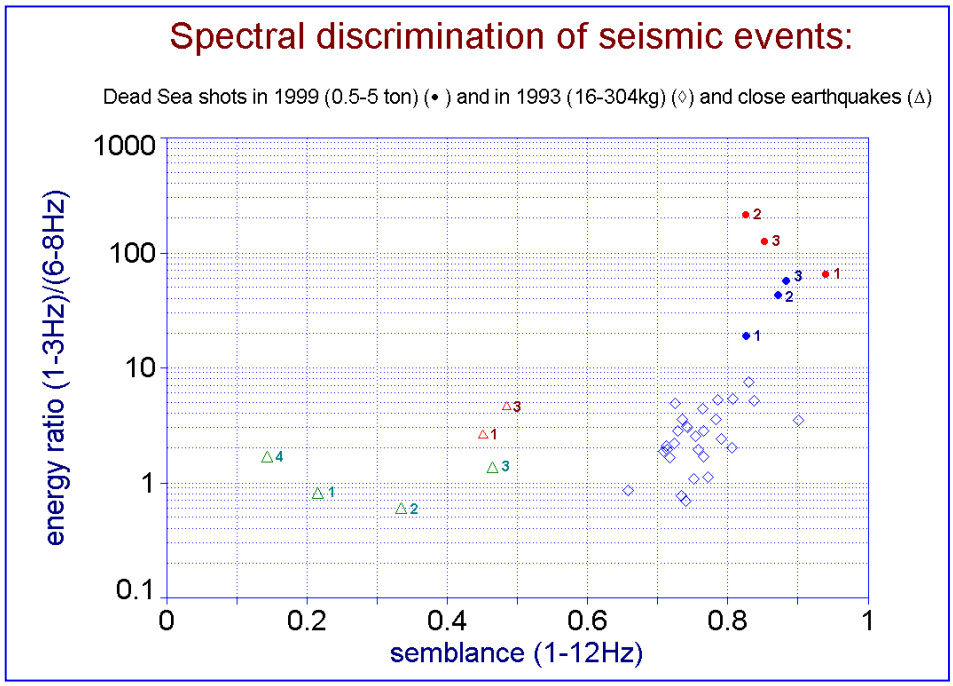

Fig. 11. Discrimination results for the Dead Sea explosions (•) and nearby earthquakes (Δ), based on ISN short-period recordings, and BB stations EIL, JER and MRNI (shown by red color, where semblance is calculated in 1-9 Hz range, because for some earthquakes only 20Hz records were available).

CONCLUSIONS AND RECOMMENDATIONS

The high magnitudes under relatively low charge weights confirm a high seismic efficiency of underwater explosions in the Dead Sea, significantly exceeding the upper limit curve for all known chemical and nuclear explosions in hard rock. The observed magnitudes and amplitudes of seismic waves verify that the whole charge was properly detonated in all cases. Our primary estimations of the seismic efficiency were justified, and the expected magnitude (about 4) was reached. Further work in estimating the seismic energy of the Dead Sea explosions is needed by the method, based on the coda envelops using broad band data at different frequency ranges.

A prominent spectral modulation (azimuth- and time-independent), caused by the bubble pulsation effect, is observed in all SP and BB seismograms, presented by the clear frequency banding in smoothed amplitude spectra of the whole signal and in spectrograms. The bubble periods, determined from the harmonic series on smoothed spectra of ISN seismograms, are in good agreement with the known empirical equation.

A preliminary discrimination analysis based on spectral energy ratio and semblance characteristics, using local short-period stations recordings of the explosions and nearby earthquakes with comparable magnitudes. Due to the specific features of seismic waves from the underwater explosions (spectra coherency at different stations, caused by the bubbling modulation, and low-frequency seismic energy), the analysis provided reliable separation between earthquakes and explosions in the Dead Sea region. Further analysis is needed including more distant seismic stations.

REFERENCES

Event Report – Dead Sea Calibration Explosions, 1999/11/08-1999/11/11, Issued: November, 1999, Center for Monitoring Research, Arlington.

Gitterman, Y., Z. Ben Avraham and A.Ginzburg, 1998. Spectral analysis of underwater explosions in the Dead Sea. Geophys. J. Int., 134, 460-472.

Gitterman Y., 1998. Magnitude-yield correlation and amplitude attenuation of chemical explosions in the Middle East. Proceedings of the 20th Annual Seismic Research Symposium on Monitoring a Comprehensive Nuclear Test Ban Treaty, Santa Fe, Sept.21-23, 1998, 302-311.

Gitterman, Y., V.Pinsky and A.Shapira, 1998. Spectral classification methods in monitoring small local events by the Israel seismic network. Journal of Seismology, 2: 237-256.

Gitterman, Y. and A. Shapira, 2000. Audio-visual and hydroacoustic observations of the Dead Sea calibration experiment, Proceedings of the 22nd Annual Seismic Research Symposium on Monitoring a Comprehensive Nuclear Test Ban Treaty, this volume.

Hofstetter, A. and Shapira, A., 2000. Determination of earthquake energy release in the Eastern Mediterranean region, Geophys. J. Int., in press.

Kanamori, H., Mori, J., Hauksson, E., Heaton, T., Hutton, K. and Jones, L., 1993. Determination of earthquakes energy release and M_L using TERRAscope, Bull. seism. Soc. Am., 83, 330-346.

Khalturin, V., T. Rautian, P. Richards and W-Y. Kim, 1997. Evaluation of chemical explosions and methods of discrimination for practical seismic monitoring of a CTBT, Report AFRL-VS-HA-TR-98-0012.

Mayeda, K. and Walter, R., 1996. Moment, energy, stress drop, and source spectra of Western United States earthquakes from regional coda envelopes, J. Geophys. Res., 101, 11195-11208.

Willis, D.E., 1963. Seismic measurements of large underwater shots, Bull. Seism. Soc. Am., 53, 789.